Formulating Wideband Array-Pattern Optimizations

Dan P. Scholnik and Jeffrey O. Coleman

scholnik@nrl.navy.mil | Naval Research Laboratory, Radar Division
jeffc@alum.mit.edu | Washington, DC 20375-5336

Abstract—Custom design of wideband digital array patterns requires a systematic approach to mapping design specifications to a program understandable by optimization engines. We show that, like in the narrowband case, wideband array patterns are closely related to multidimensional FIR filter responses, suggesting the adaptation of powerful and efficient filter design techniques to the array problem. Previously reported FIR filter design techniques are then applied to an example array-pattern design.

I. Introduction

With the continued evolution of computing power, wideband digital antenna arrays have traversed the chasm between yesterday's impracticality and today's reality. Increasingly, the traditional analog delay elements are being replaced with digital filters operating on data sampled at each element. The accompanying increase in computation complexity is offset by the precision and flexibility inherent in DSP. Fully realizing the power of a digital implementation, however, requires calculating optimal filter coefficients custom tailored to the system at hand. The powerful and efficient optimization engines [1], [2] that are required exist and often have convenient interfaces to the popular MATLAB software. What remains is to transform design specifications into a form usable by the engines.

The goal of this paper is not to argue for particular constraint choices or design strategies, as in [3], but rather to illustrate approaches to efficiently mapping common constraints to a form suitable for passing to a convex programming engine. This framework extends previous results derived for the design of single [4], [5] and multidimensional [6] FIR filters and narrow- [7] and wideband [8] arrays. In the sequel we derive the wideband array pattern and show how pattern design relates to the design of FIR filters. We then use a sample design to demonstrate the construction of an optimization program from design specifications.

II. Array Pattern Definition

Consider, as a function of position $\boldsymbol{x}$ and time t, the complex field $U(\boldsymbol{x},t) = e^{j2\pi(-\boldsymbol{v}\cdot\boldsymbol{x}+ft)}$ of a monochromatic plane wave with spatial frequency (propagation direction) vector $\boldsymbol{v}$ and temporal frequency f. The Helmholtz equation relates spatial and temporal frequencies by $|f| = c\|\boldsymbol{v}\|$, where c is the speed of propagation, but it will be convenient to defer enforcement of this constraint until later. The output of an antenna element at position $\mathbf{x}$ is then the time function $y(t) = G(\boldsymbol{v},f)U(\mathbf{x},t)$, where $G(\boldsymbol{v},f)$ is the complex gain of the element as a function of spatial and temporal frequency. The summed output of an array of multiple elements located at positions $\mathbf{x} \in \mathcal{X}$ is then

$$s(t) = \sum_{\mathbf{x}\in\mathcal{X}} G_{\mathbf{x}}(\boldsymbol{v},f)U(\mathbf{x},t)$$

We now define the array pattern as a function of $\boldsymbol{v}$ and f to be the ratio of the array output to the output $U(\mathbf{0},t)$ of an isotropic element located at the origin:

$$H(\boldsymbol{v},f) = \sum_{\mathbf{x}\in\mathcal{X}} G_{\mathbf{x}}(\boldsymbol{v},f)e^{-j2\pi\boldsymbol{v}\cdot\mathbf{x}}. \tag{1}$$

This can be viewed as the Fourier transform on the four dimensional spatio-temporal variables $(\boldsymbol{x},t)$ to transform variables $(\boldsymbol{v},f)$ of

$$h(\boldsymbol{x},t) = \sum_{\mathbf{x}\in\mathcal{X}} g_{\mathbf{x}}(\boldsymbol{x}-\mathbf{x},t), \tag{2}$$

which is often a convenient way to visualize the relationship between array geometry and the array pattern.

Equation 1 is defined for all values of $(\boldsymbol{v},f)$, which corresponds to the response to plane waves propagating at all speeds $c \in [0,\infty)$. Usually we are interested only in the array response to incident plane waves traveling at the speed of propagation c in free space, obtained by restricting the domain to the cone defined by $|f| = c\|\boldsymbol{v}\|$. The more general characterization is convenient due to the Fourier transform relationship between the array pattern and the spatial and temporal definition of the array.

Although spatial frequency vector $\boldsymbol{v}$ is convenient mathematically for specifying points on the array pattern, in practice array specifications are given from the array's perspective in terms of normalized look vector $\boldsymbol{l}/\|\boldsymbol{l}\| = -\boldsymbol{v}/\|\boldsymbol{v}\|$ or in terms of angular offsets from a reference direction. Restricting our attention to two spatial dimensions provides the simplest meaningful visualization of the cone $|f| = c\|\boldsymbol{v}\|$ (shown in Fig. 1(a)) that defines the domain of physical plane wave parameters. At any given frequency f, look vector $\boldsymbol{l}$ lies on a circle of radius $|f|/c = 1/\lambda$, corresponding to a 360° field of view from the array. Defining angle θ by $\sin(\theta) = l_x/\|\boldsymbol{l}\|$, we see that on a semicircle (Fig. 1(b)) either θ or l_x uniquely defines $\boldsymbol{l}$. (In three dimensions the circle becomes a spherical surface with two angles uniquely identifying $\boldsymbol{l}$ on a hemisphere.)

This work was supported by the Office of Naval Research through its program in Operations Research and through its Base Program at the Naval Research Laboratory.

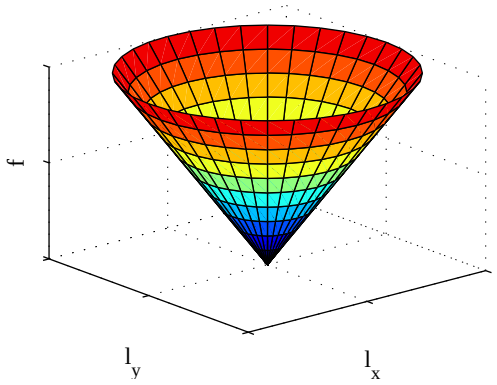

(a) The cone of physical look directions.

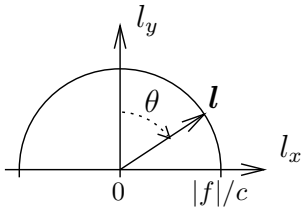

(b) A two-dimensional slice at one frequency.

Fig. 1. Restricting the array-pattern domain.

III. An Example Design

In this section we present an example design similar to that in [3] to illustrate some of the possible types of specifications for wideband array patterns. We will restrict out attention to a linear array of isotropic antenna elements uniformly located along the x-axis of a two-dimensional space, reducing the total dimension of $(\boldsymbol{x}, t)$ to three and simplifying visualization.

The frequency response at each element is assumed to be that of an FIR filter, the set of which are to be designed. Without substantial loss of generality, let the set of element locations be $\mathcal{X} = \{kd\mathbf{e_1} : k = -K, \ldots, K\}$ and the set of filter delays be $\mathcal{T} = \{nT : n = -N, \ldots, N\}$, with unit vector $\mathbf{e_1} = (1,\ 0)^T$. The array pattern is then

$$H(\boldsymbol{v}, f) = \sum_k \sum_n c_{k,n} e^{-j2\pi(kv_x d + nfT)}, \qquad (3)$$

where $\boldsymbol{v} = (v_x,\ v_y)^T$. This is the response of a two-dimensional FIR filter in three dimensions and is not a function of v_y since the array has no extent in the y dimension. The array pattern is periodic in the other two directions, with period $1/T$ in frequency f and period $1/d$ in spatial frequency v_x. Usually we want the total range of v_x to be no greater than $1/d$, so that the pattern can be uniquely specified for all look directions, thus avoiding undesired grating lobes. Since a 180° field of view at positive frequency f corresponds to $v_x \in [-f/c, f/c]$, this requires the familiar $d \le c/2f = \lambda/2$ for the highest frequency of interest. Likewise, $1/T$ should be chosen larger than the desired instantaneous bandwidth of the array. Of particular importance is that (3) is linear in the coefficients $\{c_{k,n}\}$ (and would be even with arbitrary element locations), permitting many common constraints to be expressed as upper bounds of convex functions of the coefficients. This in turn allows design of the array pattern using convex optimization tools [9], [10], [4]

Since the element locations and filter delays are symmetrically located, if the FIR filter coefficients obey the symmetry $c_{-k,-n} = c_{k,n}^*$, then the array pattern (3) is real-valued (a linear-phase response). This not only reduces by one half the number of variables to optimize but can be exploited to reduce real-time computation requirements as well. Unless a specific (nonlinear) phase response is desired, these significant benefits come with no ill effects.

The example system parameters are as follows. The RF center frequency is 1.25 GHz, the system bandwidth is $B = 400$ MHz, and the data rate is $1/T = 500$ MHz. The array is composed of 15 identical isotropic elements, each feeding an 11-tap, complex-coefficient, nonlinear-phase FIR filter with the filters obeying the symmetry discussed above. The spacing D between the elements is one half wavelength at the highest in-band frequency of 1.45 GHz in order to suppress grating lobes at all in-band frequencies. The pattern is designed to point to 45°.

The specifications for the optimization follow, representing the pattern as an explicit function of angle θ:

$$\begin{aligned}
&\text{min. } \alpha \\
&\text{s.t. } \int_{f\in\mathcal{F}_{\text{pb}}} \int_{\theta\in\Theta_{\text{sl}}} |H(\theta, f)|^2 \, d\theta \, df \le \alpha && (4)\\
&\quad |H(\theta, f)| \le 10^{-25/20},\ \theta \in \Theta_{\text{sl}},\ f \in \mathcal{F}_{\text{pb}} && (5)\\
&\quad \frac{1}{B}\int_{f\in\mathcal{F}_{\text{pb}}} |H(\theta_m, f) - \beta_m|^2 \, df \le 10^{-50/10}, \\
&\qquad\qquad\qquad\qquad m = 1, \ldots, M && (6)\\
&\quad \frac{1}{M}\sum_m \beta_m = 1 && (7)\\
&\quad \sum_k \sum_n |c_{k,n}|^2 \le \epsilon && (8)
\end{aligned}$$

The optimization was performed in a few minutes using a convex programming engine [1] under MATLAB. The resulting response of the array pattern versus angle and frequency is shown in Fig. 2. The following sections explore the purpose and construction of the above specifications.

A. Sidelobe constraints

The sidelobe region is shown as the shaded region in Fig. 3(a). It consists of a full 180° field of view over the entire band minus a constant width in angle. Constraints (4) and (5) limit the L_2 and L_∞ norms over this region. The L_∞ constraint, ensuring all sidelobes lie below -25 dB, (5) is straightforward to construct. We grid along both frequency and angle, and at each grid point in the sidelobe region two linear constraints are used to bound the

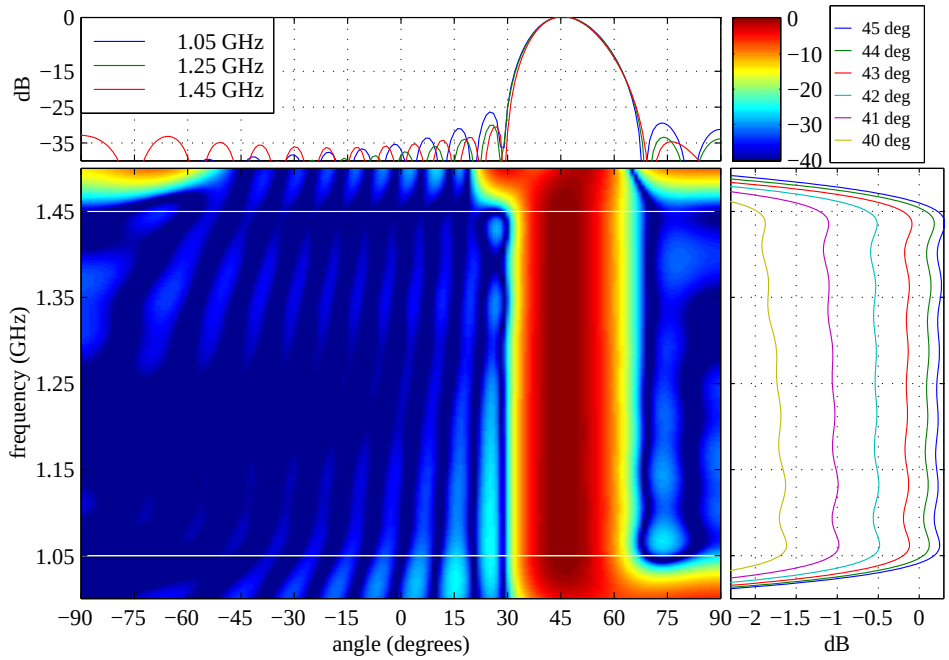

Fig. 2. Optimized wideband array pattern. The upper-left plot shows cuts across angle, and the lower-right plot show cuts across frequency.

magnitude of the (real) response. The grid spacing is chosen small enough that the array pattern cannot exceed the bound significantly between the grid points. For this example, experimentation yielded a grid spacing of $1/32T$ in f and approximately $1/128D$ in v_x.

Constraint (4) and the linear objective α together minimize the energy (squared L_2 norm) in the sidelobes, subject to the other constraints. The left side of (4) represents a quadratic form in the FIR coefficients, but it requires computation of the integral to find the quadratic kernel needed by the optimizer. This could be approximated by a double Riemann sum on a grid, with the resulting tradeoff between grid density (computation) and accuracy. Here we choose a intermediate approach. We use the test-input approach of [5] to formulate the inner integral exactly, while approximating the outer integral with a summation.

At any fixed frequency f, (3) represents the response in the variable v_x of a one-dimensional FIR filter with coefficients that are linear combinations of the array coefficients $\{c_{k,n}\}$. If we consider a zero-mean, wide-sense stationary spatial random process input with temporal frequency f and spectral density $S_{\text{in}}(v_x, f)$, the output power is

$$P_{\text{out}}(f) = \int |H(v_x, f)|^2 S_{\text{in}}(v_x, f)\, dv_x. \qquad (9)$$

The resulting quadratic kernel can be computed exactly and efficiently when the input density is specified in terms of weighted and shifted basis functions as detailed in [5]. To obtain the inner integral of (4), choose

$$S_{\text{in}}(v_x, f) = \begin{cases} \frac{c}{f\cos(\theta)}, & -\theta \in \Theta_{\text{sl}} \\ 0, & \text{otherwise.} \end{cases}$$

which effects the change of variable $v_x = -\sin(\theta) f/c \rightarrow \theta$. The double integral is now approximated by the sum

$$\begin{aligned} P_{\text{out}} &= \sum_i \int |H(v_x, f_i)|^2 S_{\text{in}}(v_x, f_i)\, dv_x\, \Delta f \\ &= \sum_i \int_{\theta \in \Theta_{\text{sl}}} |H(\theta, f_i)|^2\, d\theta\, \Delta f \end{aligned}$$

over the grid of frequencies $\{f_i\}$ with spacing Δf.

B. Mainbeam Constraints

Figure 3(b) is a blowup of the mainbeam cutout region of Fig. 3(a). The central shaded region represents angles at which we wish to control the frequency response of the array. We want the frequency response at each angle on the shaded portion of the grid (indicated by the vertical lines) to be flat while still allowing the beam to rolloff with angle. To accomplish this we allocate auxiliary variables $\{\beta_m\}$, one for each angle, to act as floating nominal-gain levels. For each angle then we approximate the left-hand side of (6) with the Riemann sum

$$\sum_i |H(\theta_m, f_i) - \beta_m|^2 \Delta f$$

over the grid of frequencies $\{f_i\}$ with spacing Δf. The resulting constraints ensure that the frequency response at each angle θ_m closely approximates β_m. The average mainlobe gain is then found by averaging the $\{\beta_m\}$, leading to a single linear equality constraint (7).

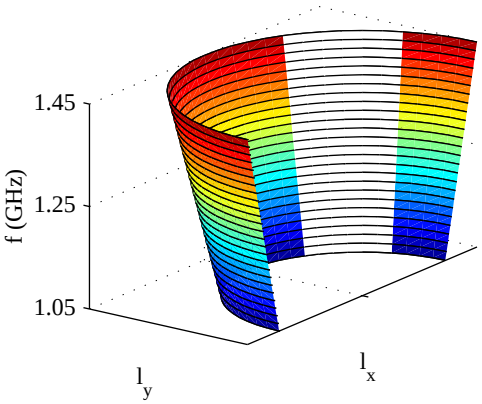

(a) The sidelobe constraint region. The horizontal lines on the shaded region represent the power distributions of narrowband spatial inputs on a grid of frequencies.

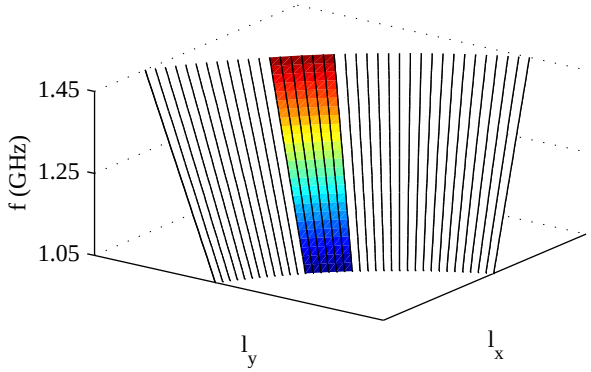

(b) A blowup of the mainbeam cutout. The mean square frequency response error along each vertical line in the shaded region and the average of the nominal gains for each are constrained.

Fig. 3. Sidelobe and mainbeam constraint regions.

C. Nonvisible Sidelobe Constraint

Constraints (4) and (5) both limit the array pattern over the sidelobe region corresponding to a 180° angular extent (the visible region) for in-band frequencies. By design, this region lies within one period of the array-pattern response. Shown in Fig. 4 is the projection of the visible region onto a $1/D$-by-$1/T$ rectangle in the (l_x, f) plane. The white region, comprised of the out-of-band and nonvisible regions, is not directly constrained, possibly resulting in extreme behavior of the array pattern. While this will not affect the response to an in-band plane wave, it will affect receiver noise. A simple solution is to limit the total power resulting from white inputs to the FIR filter of each element. A modest limit will prevent extreme responses but have minimal effect on the visible region. Constraint (8) then results from applying Parseval's relation to obtain a simpler expression for this special case.

IV. Conclusions

We have shown that under appropriate conditions the response of a wideband array can be seen as a four-dimensional Fourier transform, complicated by the restriction of the four-dimensional spatio-temporal frequency to a four-dimensional cone, effectively removing one dimension. The remaining three dimensions are equivalent in combination to temporal frequency and the two usual spatial pointing angles. This result suggests adapting filter design strategies to array design, particularly efficient ways to calculate the quadratic kernel on an L_2 constraint. In the example we adapted the test-input approach for L_2 constraints [5] to reduce a two-dimensional Riemann sum to a one-dimensional sum of exact integrals. This can be extended to multidimensional test inputs (as in [8]) to avoid gridding at all, with the caveat that the required autocorrelation functions can become difficult to compute exactly.

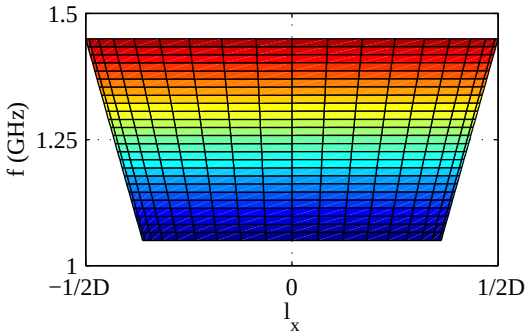

Fig. 4. Projecting the cone onto the (l_x, f) plane shows the nonvisible response region (in white).

References

[1] J. F. Sturm, "Sedumi," MATLAB toolbox, May 1998, `http://www.unimaas.nl/~sturm/software/sedumi.html`.

[2] R. Vanderbei, "LOQO: An interior point code for quadradic programming," Technical Report SOR 94-15, Princeton University, 1994, revised 11/30/98, to appear in *Optimization Methods and Software*.

[3] D. P. Scholnik and J. O. Coleman, "Optimal design of wideband array patterns," in *Proc. 2000 IEEE Int'l Radar Conference*, Washington, DC, May 2000, Accepted for publication.

[4] J. O. Coleman and D. P. Scholnik, "Design of nonlinear-phase FIR filters with second-order cone programming," in *Proc. Midwest Symp. on Circuits and Systems (MWSCAS)*, Las Cruces, NM, Aug. 1999.

[5] J. O. Coleman, "Systematic mapping of quadratic constraints on embedded FIR filters to linear matrix inequalities," in *Proc. 1998 Conference on Information Sciences and Systems (CISS '98)*, Princeton, NJ, Mar. 1998.

[6] W.-S. Lu and A. Antoniou, "Design of nonrecursive 2-D digital filters using semidefinite programming," in *Proc. 1999 Int'l Symp. Circuits and Systems (ISCAS '99)*, Orlando, FL, May 1999.

[7] H. Lebret and S. Boyd, "Antenna array pattern synthesis via convex optimization," *IEEE Trans. on Signal Processing*, vol. 45, no. 3, pp. 526–32, Mar. 1997.

[8] J. O. Coleman and R. J. Vanderbei, "Random-process formulation of computationally efficient performance measures for wideband arrays in the far field," in *Proc. Midwest Symp. on Circuits and Systems (MWSCAS)*, Las Cruces, NM, Aug. 1999.

[9] L. Vandenberghe and S. Boyd, "Semidefinite programming," *SIAM Review*, vol. 38, no. 1, pp. 49–95, Mar. 1996.

[10] M. S. Lobo, L. Vandenberghe, S. Boyd, and H. Lebret, "Applications of second-order cone programming," *Linear Algebra and its Applications*, vol. 284, pp. 193–228, Nov. 1998.